# The Xylem and Phloem Transcriptomes from Secondary Tissues of the Arabidopsis Root-Hypocotyl[1][w]

**Chengsong Zhao, Johanna C. Craig, H. Earl Petzold, Allan W. Dickerman, and Eric P. Beers***

Department of Horticulture (C.Z., H.E.P., E.P.B.) and Virginia Bioinformatics Institute (J.C.C., A.W.D.), Virginia Polytechnic Institute and State University, Blacksburg, Virginia 24061

The growth of secondary xylem and phloem depends on the division of cells in the vascular cambium and results in an increase in the diameter of the root and stem. Very little is known about the genetic mechanisms that control cambial activity and the differentiation of secondary xylem and phloem cell types. To begin to identify new genes required for vascular cell differentiation and function, we performed genome-wide expression profiling of xylem and phloem-cambium isolated from the root-hypocotyl of Arabidopsis (*Arabidopsis thaliana*). Gene expression in the remaining nonvascular tissue was also profiled. From these transcript profiles, we assembled three sets of genes with expression significantly biased toward xylem, phloem-cambium, or nonvascular tissue. We also assembled three two-tissue sets of genes with expression significantly biased toward xylem/phloem-cambium, xylem/nonvascular, or phloem-cambium/nonvascular tissues. Localizations predicted by transcript profiles were supported by results from promoter-reporter and reverse transcription-polymerase chain reaction experiments with nine xylem- or phloem-cambium-biased genes. An analysis of the members of the phloem-cambium gene set suggested that some genes involved in regulating primary meristems are also regulators of the cambium. Secondary phloem was implicated in the synthesis of auxin, glucosinolates, cytokinin, and gibberellic acid. Transcript profiles also supported the importance of class III HD ZIP and KANADI transcription factors as regulators of radial patterning during secondary growth, and identified several members of the G2-like, NAC, AP2, MADS, and MYB transcription factor families that may play roles as regulators of xylem or phloem cell differentiation and activity.

Xylem and phloem, the two conducting tissues of the plant vascular system, are of tremendous fundamental interest and economic importance. Xylem is the water-conducting tissue, and secondary xylem provides the raw material for the forest products industry. The efficiency of amino acid and Suc transport through the phloem affects the growth and quality of sink tissues. The movement of signaling molecules through the phloem is a crucial component of systemic adaptation to the environment and regulation of growth and development (Ruiz-Medrano et al., 2001). In addition to their roles as conducting tissues, xylem and phloem have important mechanical, storage, and secondary metabolic roles.

Genes identified through forward genetic screens for vascular tissue mutants (for review, see Ye, 2002) span a wide range of functional categories, including, for example, signal perception/transduction (Scheres et al., 1995; Mahonen et al., 2000; Inoue et al., 2001; Clay and Nelson, 2002; Carland and Nelson, 2004), auxin transport (Galweiler et al., 1998), auxin-mediated transcriptional regulation (Hardtke and Berleth, 1998), and cellulose biosynthesis (Gardiner et al., 2003). Levels of vascular tissue development affected in these mutants include cell, tissue, and organ (vascular patterning) phenotypes. To date, only one mutant, *apl*, has been reported to exhibit widespread absence of a subset of vascular cell types. Roots of *apl* seedlings lack both sieve elements (SEs) and companion cells (CCs; Bonke et al., 2003). Additional mutations that specifically eliminate other vascular cell types (i.e. cambium cells, tracheary elements [TEs], and vascular parenchyma cells or fibers) are needed to identify and characterize genetic mechanisms that control vascular cell fate. The availability of comprehensive xylem, cambium, and phloem transcript profiles would facilitate reverse genetic studies of vascular tissue development and provide a valuable complement to forward genetic screens for vascular tissue mutants.

Six model systems, loblolly pine (*Pinus taeda*), poplar (*Populus* spp.), Zinnia, celery (*Apium graveolens*), Eucalyptus, and Arabidopsis (*Arabidopsis thaliana*), have been used for transcriptome analyses of isolated vascular tissues or cultured TEs. Xylem expression profiling via expressed sequence tag analysis was conducted for loblolly pine (Allona et al., 1998) and poplar (Sterky et al., 1998). An expanded poplar expressed sequence tag set formed the basis for a recent microarray analysis of cambium, phloem, and radially expanding xylem (Schrader et al., 2004). Microarray (Demura et al., 2002) and cDNA-amplified

[1] This work was supported by the National Science Foundation (grant no. IBN–0131386 to E.P.B.), the Department of Energy (grant no. DE–FG02–04ER15627 to E.P.B.), and the Virginia Tech ASPIRES program (grant no. 232500 to A.W.D. and E.P.B.).

* Corresponding author; e-mail ebeers@vt.edu; fax 540–231–3083.

[w] The online version of this article contains Web-only data.

Article, publication date, and citation information can be found at www.plantphysiol.org/cgi/doi/10.1104/pp.105.060202.

fragment length polymorphism analyses (Milioni et al., 2002) were used to profile expression during the differentiation of cultured Zinnia TEs. A 1,326-clone macroarray based on a cDNA library from the isolated phloem of celery was used to identify new genes important to phloem (Vilaine et al., 2003). Xylem transcript profiling using a cDNA array developed from a xylem-subtractive library was recently conducted for Eucalyptus secondary xylem (Paux et al., 2004). The transcriptomes of xylem and bark isolated from the root-hypocotyl of Arabidopsis were profiled using the partial genome, 8 K Affymetrix GeneChip (Oh et al., 2003), and transcripts of the inner stele of the seedling root were recently profiled using the 24 K Affymetrix ATH1 Arabidopsis Genome Array (24 K GeneChip; Birnbaum et al., 2003). While the aforementioned vascular tissue transcriptome studies represent important advances, genome-wide transcript profiles of isolated secondary xylem and phloem are needed for a comprehensive approach to the functional genomics of vascular tissue differentiation and function.

For the transcript profiling described in this report, we used the 24 K GeneChip that provides approximately 90% genome coverage of annotated genes. We also have increased the tissue resolution compared to earlier studies with Arabidopsis xylem and bark (Zhao et al., 2000; Oh et al., 2003) by further dissecting the bark to separate phloem-cambium and nonvascular peripheral tissues (Fig. 1). From the transcriptomes of these three tissue samples, we have assembled three one-tissue gene sets for xylem (X), phloem-cambium (PC), and nonvascular (NV) and three two-tissue gene sets for X/PC, X/NV, and PC/NV. That wood-forming xylem and phloem-cambium were successfully isolated from one another and from the nonvascular tissue was demonstrated through the analysis of the distribution of transcripts for known vascular tissue marker genes. The reliability of the gene sets as tools for identifying new genes expressed in xylem or phloem-cambium was supported by results from promoter-reporter and reverse transcription (RT)-PCR experiments with nine novel xylem and phloem-cambium genes. Potential similarities between gene expression in apical meristems and the cambium are discussed. A comprehensive view of genes that may be required for xylem secondary cell wall biosynthesis and lignification is provided. New information regarding localization of transcripts for glucosinolate and hormone metabolism genes is presented. The potential for uncharacterized xylem and phloem-cambium G2-like, NAC, AP2 domain, MADS box, and MYB transcription factors and the CLAVATA/CLE signaling system to regulate xylem and phloem differentiation is also discussed. The gene sets assembled for this report are valuable tools for the design of reverse genetic experiments aimed at understanding secondary cell wall biosynthesis, lignification, cambium activity, and vascular cell differentiation and function.

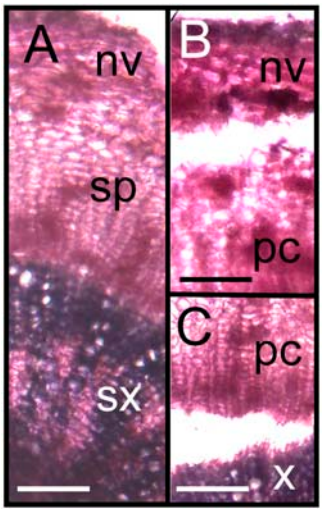


**Figure 1.** Three tissue samples can be isolated from the root-hypocotyl. A, Extensive secondary growth is evident in the root-hypocotyl of an 8-week-old Arabidopsis plant. Lignified vessels and fibers of secondary xylem are stained blue with TBO. Nonlignified primary cell walls of cells in secondary xylem, secondary phloem, and nonvascular tissues are stained pink with ruthenium red. B, Nonvascular tissue of the outer bark can be separated from secondary phloem, yielding the nonvascular sample for expression profiling. C, Secondary phloem can be separated from secondary xylem, yielding the phloem-cambium and xylem samples for expression profiling. Free-hand transverse sections were prepared from fresh tissue just prior to staining. Tissues were dissected after staining. nv, Nonvascular; pc, phloem-cambium; sp, secondary phloem; sx, secondary xylem; x, xylem. Bars = 50 $\mu$m.

## RESULTS

### Statistical Summary

Of the approximately 22,750 probe sets used on the 24 K GeneChip to interrogate approximately 23,750 Arabidopsis genes (Redman et al., 2004), the number flagged as present by Affymetrix Microarray Suite version 5.0 (''Materials and Methods'') with a signal intensity above 200 in at least one chip was 16,311. Counting only genes flagged as present in both biological replicates within a tissue, X expressed 11,440 genes, PC 12,375, and NV 13,151. Within-tissue mean signal intensities (MSI) and raw data (i.e. signal intensities and present and absent calls for all replicates) for all probes on the 24 K GeneChip can be found in Supplemental Tables I and II, respectively, which are published as supporting tables on the journal Web site.

The correlation between technical replicates, the same cRNA sample run on two chips (mean $R^2$ = 0.995), was higher than that between biological replicates (mean $R^2$ = 0.964), which was higher than the between-tissue correlations, as expected. Xylem stood out as the most distinct tissue, as the correlation between PC and NV tissue profiles was higher ($R^2$ = 0.944) than that between X and PC ($R^2$ = 0.873) and between X and NV ($R^2$ = 0.897). Analysis of variance showed significant gene effects and gene-by-tissue interaction ($P < 10^{-15}$ for both), while the effects of chips

and RNA samples were not significant. The significant gene-by-tissue interaction indicated that at least some genes have different patterns of expression across tissues. We used the SD of log ratios of biological replicates within intensity-defined bins to generate Z-scores for testing between-tissue comparisons. A total of 1,985 genes exhibited a between-tissue log ratio at least 3.29 SDs from the mean for a nominal probability of 0.001. Figure 2 presents ratio-intensity plots of each pair-wise tissue comparison using color to highlight significantly tissue-biased genes. To view three-way relationships among tissues, we plotted the data in a space that shows the relative level of expression in three tissues simultaneously in what we call a "triangle plot" (Fig. 3). Genes belonging to the six tissue-biased gene sets assembled for this report are highlighted in color on the triangle plot, where one-tissue-biased (X, PC, and NV) genes are shown in red and two-tissue-biased (X/PC, X/NV, and PC/NV) genes are shown in green.

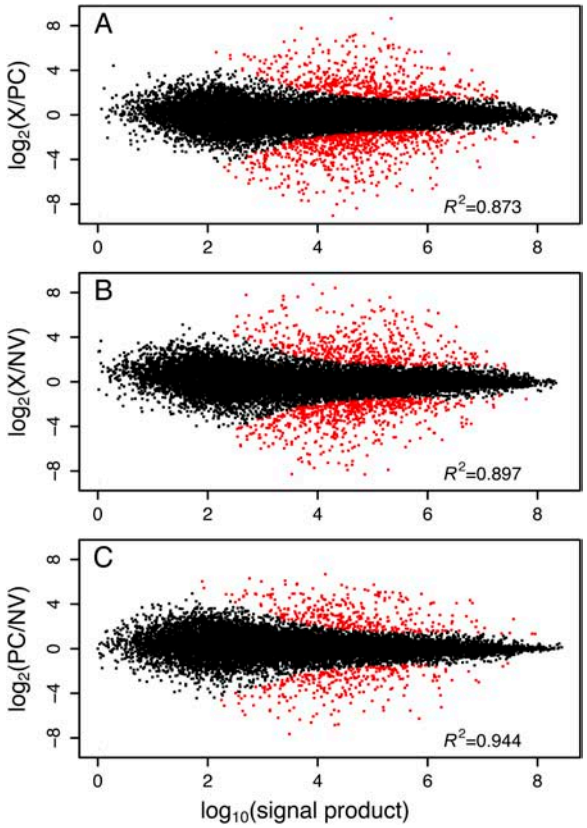


**Figure 2.** Ratio-intensity plots of between-tissue comparisons with statistically biased genes (≥3.29 SDs, $P \leq 0.001$) highlighted. The vertical axis plots the $\log_2$ of the ratio of the normalized MSIs for the same gene between two tissues: X versus PC (A), X versus NV (B), and PC versus NV (C). The horizontal scale specifies the $\log_{10}$ of the product of the two MSIs for the same gene between two tissues. Genes with between-tissue means below 50 (0.1 times the among-genes mean) were considered insignificant regardless of ratio due to the noise in that region. Correlations ($R^2$ values) are shown in the lower right corner for each between-tissue comparison.

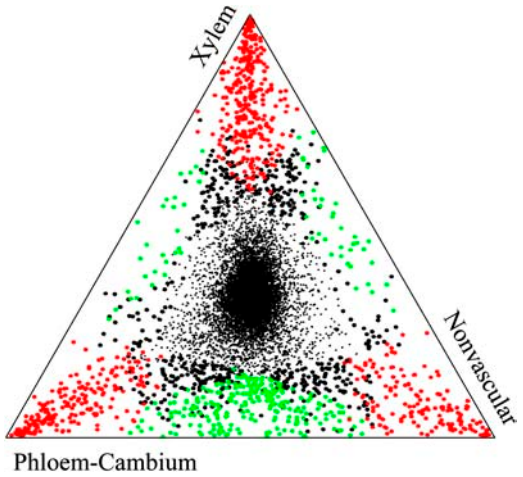


**Figure 3.** "Triangle plot" of the relative MSIs among three tissues. Each gene is represented by a point whose proximity to each of the tissue-labeled corners reflects the relative expression in that tissue (see "Materials and Methods" for the numerical formula). Only genes with MSI values ≥200 are shown. Genes expressed in a single tissue lie in an extreme corner, while those expressed equally in all three lie in the center. Genes with signals significantly ($P \leq 0.001$) higher in one tissue relative to both other tissues are highlighted in red (so-called "one-tissue genes"). Genes with signals not significantly different for two tissues but higher in both of those tissues relative to the third are highlighted in green (so-called "two-tissue genes"). Genes with signals significantly biased in only one pair-wise comparison or those not significantly biased in any pair-wise comparison are shown as large and small black points, respectively.

### Expression of Previously Characterized Markers for Xylem, Phloem, and Nonvascular Tissues

#### *Xylem Markers*

To assess the level of purity of isolated tissues, we used previously characterized tissue-specific markers. Marker gene expression ratios ($\log_2$ of the ratio of the MSIs for the three pair-wise tissue comparisons, X versus PC, X versus NV, and PC versus NV) are presented in Table I. Parenchyma cells, TEs, and fibers are visible in secondary xylem of Arabidopsis hypocotyls (Chaffey et al., 2002). Markers specific to Arabidopsis xylem parenchyma and fibers have not yet been reported. The xylem markers considered here are associated with TEs synthesizing secondary cell walls. The xylem cellulose synthase (CesA) genes, *IRX1* (*CesA8*, At4g18780), *IRX3* (*CesA7*, At5g17420) and *IRX5* (*CesA4*, At5g44030), were identified from irregular xylem (*irx*) mutants (Taylor et al., 2003) and are coexpressed in xylem vessels (Gardiner et al., 2003). XCP1 and XCP2 are the two Arabidopsis Cys proteases sharing the highest degree of identity with the Zinnia TE protease p4817 (Ye and Varner, 1996; Beers et al., 2004), and XCP1 has been localized to Arabidopsis TEs (Funk et al., 2002). For all xylem markers, expression was significantly ($P < 0.001$) X biased with $\log_2$ values for X versus PC or X versus NV ratios of MSIs ranging from 3.8 to 6.8 (Table I).

**Table I.** *Relative signal intensities and tissue biases for known Arabidopsis marker genes for xylem, phloem, or nonvascular peripheral cells*

| Locus | Gene Symbol | Description | $Log_2$ (X versus PC)[a] | $Log_2$ (X versus NV) | $Log_2$ (PC versus NV) | Tissue Bias, This Report | Published Localization | Reference |
|---|---|---|---|---|---|---|---|---|
| At4g18780 | IRX1 | Cellulose synthase catalytic subunit | 4.7* | 3.8* | −0.9 | X | Xylem TEs | Gardiner et al. (2003) |
| At5g17420 | IRX3 | Cellulose synthase catalytic subunit | 4.1* | 4.1* | 0.0 | X | Xylem TEs | Gardiner et al. (2003) |
| At5g44030 | IRX5 | Cellulose synthase catalytic subunit | 4.0* | 4.1* | 0.1 | X | Xylem TEs | Gardiner et al. (2003) |
| At4g35350 | XCP1 | Cys proteinase | 6.8* | 6.2* | −0.6 | X | Xylem TEs | Funk et al. (2002) |
| At1g20850 | XCP2 | Cys proteinase | 6.2* | 6.5* | 0.3 | X | Xylem TEs | Funk et al. (2002) |
| At5g57350 | AHA3 | Plasma membrane ATPase 3 (proton pump) | −6.0* | −1.2 | 4.8* | PC | Phloem CCs | DeWitt and Sussman (1995) |
| At1g79430 | APL | G2-like transcription factor | −6.2* | −1.4 | 4.8* | PC | Phloem SE/CCs | Bonke et al. (2003) |
| At1g05760 | RTM1 | Jacalin lectin family protein | −4.2* | 1.5 | 5.8* | PC | Phloem SEs | Chisholm et al. (2001) |
| At1g22710 | SUC2 | Suc transporter/ Suc-proton symporter | −3.4* | 0.7 | 4.0* | PC | Phloem CCs | Stadler and Sauer (1996) |
| At1g12110 | NRT1.1/ CHL1 | Nitrate/chlorate transporter | −0.8 | −3.5* | −2.6* | NV | Epidermis (hypocotyl guard cells) | Guo et al. (2003) |
| At1g08090 | NRT2.1 | High-affinity nitrate transporter | −1.3 | −6.1* | −4.9* | NV | Endodermis, cortex, epidermis | Nazoa et al. (2003) |

[a]$Log_2$ of the signal ratio for the three pair-wise tissue comparisons (X versus PC, xylem versus phloem-cambium; X versus NV, xylem versus nonvascular, PC versus NV, phloem-cambium versus nonvascular), where a positive value indicates a higher signal for the first member of the pair-wise comparison and a negative value indicates a higher signal for the second member of the pair-wise comparison. $Log_2$ values representing pair-wise comparisons between significantly different signals are indicated by a single asterisk. For reference: a $log_2$ value of 4 is equivalent to a 16-fold difference between signals, while a $log_2$ value of 6 is equivalent to a 64-fold difference between signals.

### *Phloem Markers*

Secondary phloem in the Arabidopsis hypocotyl contains sieve-tube elements, CCs, parenchyma cells, and fibers (Chaffey et al., 2002). Markers for Arabidopsis phloem parenchyma and phloem fibers have not yet been reported. However, reliable markers are available for SEs and/or CCs. Two markers for phloem CCs in Arabidopsis are the Suc-$H^+$ symporter SUC2 (At1g22710; Stadler and Sauer, 1996) and the plasma membrane proton pump ($H^+$-ATPase) AHA3 (At5g57350; DeWitt and Sussman, 1995). RTM1 (At1g05760), a protein that restricts the long-distance movement of tobacco etch virus (Chisholm et al., 2001), and APL (At1g79430), a phloem G2-like transcription factor required for SE differentiation (Bonke et al., 2003), are more recently characterized markers for SEs. For all phloem markers, expression was significantly PC-biased with absolute $log_2$ values for ratios of PC MSIs compared with X or NV MSIs ranging from 3.4 to 6.2 (Table I).

### *Nonvascular Markers*

With extensive secondary growth, the nonvascular tissue of the root-hypocotyl consists largely of cork cells (Kondratieva-Melville and Vodolazsky, 1982; Dolan and Roberts, 1995), and those in the outermost layers may be suberized (Chaffey et al., 2002). Pericycle cells form the boundary between the secondary phloem and the cork cambium and cork (Busse and Evert, 1999). This boundary is less distinct than the X-PC boundary (Fig. 1A). No information is available on markers for secondary pericycle or cork. Hence, the selection of nonvascular markers *NRT1.1/CHL1* and *NRT2.1* for this study was based on their expression patterns in young root-hypocotyl tissue. NRT1.1/CHL1 (At1g12110) and NRT2.1 (At1g08090) are nitrate transporters (Orsel et al., 2002; Guo et al., 2003). *NRT1.1* is expressed in guard cells of mature leaves and hypocotyls (Guo et al., 2003). *NRT2.1* is the most highly expressed member of the *NRT2* family from Arabidopsis, and a *NRT2.1* promoter-$\beta$-glucuronidase (GUS) fusion was expressed in all cells outside of the stele (Nazoa et al., 2003). For these nonvascular markers, expression in isolated secondary tissues was significantly NV-biased with absolute $log_2$ values for ratios of NV MSIs versus X or PC MSIs ranging from 2.6 to 6.1 (Table I).

### Expression of Previously Characterized Cambium and Apical Meristem Markers

Cambium and radially expanding xylem cells were shown to partition with bark separated from second-

ary xylem of hybrid aspen (Gray-Mitsumune et al., 2004). To determine whether cambium and radially expanding xylem cells partitioned with xylem or phloem isolated from the Arabidopsis root-hypocotyl, we considered the expression patterns of Arabidopsis homologs or orthologs of recently reported cambium and radially expanding xylem markers from aspen. The subgroup A $\alpha$-expansin *PttEXP1* is a marker for cambium and radially expanding xylem in aspen (Gray-Mitsumune et al., 2004). In the Arabidopsis root-hypocotyl, two PC-biased $\alpha$-expansins, *EXPA9* (At5g02260) and *EXPA10* (At1g26770), were noted (Supplemental Table IV). *EXPA9* belongs to subgroup A of $\alpha$-expansins (Gray-Mitsumune et al., 2004). Cambial expression of poplar genes *PttANT* and *PttCLV1*, predicted orthologs of *ANT* (At4g37750) and *CLV1* (At1g75820), was recently reported (Schrader et al., 2004). The receptor kinase gene *CLV1* restricts the size of the pool of undifferentiated cells in the shoot and flower apical meristems (for review, see Carles and Fletcher, 2003). In the root-hypocotyl, *CLV1* was a PC-biased gene (Table II). *ANT*, a positive regulator of meristematic activity (Mizukami and Fischer, 2000), was also found to be a PC-biased gene (Table II). Based on the vascular cambium expression reported for *PttEXP1*, *PttCLV1*, and *PttANT* and the fact that the samples used for this study contained no apical meristems, we conclude that the PC-biased expression of *CLV1*, *ANT*, and *EXPA9* reflects the presence of the vascular cambium, and perhaps radially expanding xylem, in the PC sample.

The high between-tissue MSI ratios reported for the tissue-specific markers listed in Tables I and II reflect very low MSIs for these genes when they are considered as negative markers from adjacent tissues (Supplemental Fig. 1). Specifically, X and NV samples contained very low levels of the phloem and cambium (i.e. negative) markers *AHA3*, *SUC2*, *RTM1*, *APL*, *ANT*, *CLV1*, and *EXPA9*, with both *APL* and *RTM1* being scored as absent from X and NV samples for both biological replicates (Supplemental Table II). Similarly, the PC sample contained very low levels of the xylem and nonvascular (i.e. negative) markers *IRX1*, *IRX3*, *IRX5*, *XCP1*, *XCP2*, *NRT2.1*, and *NRT1.1*, with *XCP1* and *NRT2.1* being scored as absent from the PC sample (Supplemental Table II). Due to the lack of published markers for the pericycle cells that form the boundary between the conducting cells of the phloem and the perivascular cork, it is not yet possible to determine the relative partitioning of pericycle cells between the PC and NV samples. Nonetheless, the distributions of transcripts for positive and negative markers for vascular cell types conformed to previously published localizations (see references listed in Table I and Gray-Mitsumune et al., 2004; Schrader et al., 2004), indicating that the X and PC transcript profiles are valuable resources for predicting novel gene expression patterns in xylem, phloem, and cambium.

**Promoter-Reporter and RT-PCR Experiments with Selected X-, PC-, and NV-Biased Genes**

To illustrate the value of X and PC gene sets as resources for the identification of new vascular tissue genes, localization studies using promoter-reporter fusions for two PC-biased and three X-biased genes are shown in Figure 4. Green fluorescent protein (GFP) driven by the *CLV1* promoter (Gallois et al., 2002) localized to the phloem and cambium in the hypocotyl (Fig. 4A). An et al. (2004) previously noted that the *CLV1* promoter was capable of driving *GUS* expression in Arabidopsis vascular tissue but did not report whether expression was xylem or phloem localized. GUS activity driven by the promoter for the most highly expressed PC-biased, G2-like transcription factor, *MYR1* (At5g18240; Thelander et al., 2002), was observed throughout the vascular system (Fig. 4D). Within the vascular tissue, GUS staining localized to the phloem in root, stem, and petiole (Fig. 4, B, C, and E). Promoter activity for the X-biased gene *ZFWD1* (At4g25440; Terol et al., 2000) was limited to vascular tissues throughout the plant and localized to xylem cells, shown here in a representative cotyledon (Fig. 4, F and G). We also tested promoter activity for the most highly expressed, X-biased NAC gene, *ANAC104* (At5g64530; Ooka et al., 2003), which we have named *XND1* (*XYLEM NAC DOMAIN 1*). GUS staining resulting from *XND1* promoter activity localized to xylem, as shown for a vessel isolated from root secondary xylem (Fig. 4H) and a metaxylem vessel adjacent to a mature protoxylem pole in a seedling root (Fig. 4J). In the shoot, *XND1p*::*GUS* activity was detected only in the vascular system of senescing leaves (Fig. 4I), i.e. *XND1p*::*GUS* activity was not detected in nonsenescing leaves or inflorescences. These results for leaf expression of *XND1p*::*GUS* are consistent with recent identification of *XND1* as a member of the leaf senescence transcriptome (Guo et al., 2004). The promoter for the most highly expressed, X-biased subtilisin-like Ser protease, At1g20160, directed expression in vascular tissue throughout the plant, as shown in a representative leaf (Fig. 4L). GUS staining in the midvein of *At1g20160p*::*GUS* plants occurred predominantly on the adaxial (xylem) side (compare GUS staining in Fig. 4K with the predominantly abaxial [phloem]-side GUS staining in Fig. 4E, driven by *MYR1p*). Thus, all five genes tested in promoter-reporter experiments yielded expression patterns consistent with those predicted by their membership in X or PC gene sets. The relevancy of the secondary X and PC transcriptomes to primary vascular tissues is supported by the observation that promoters for *MYR1*, *ZFWD1*, *XND1*, and *At1g20160* were capable of driving GUS expression in primary vascular tissues.

We used RT-PCR to evaluate five more genes that exhibited tissue-biased expression patterns. Amplification for two X-biased NAC genes (At1g02250 and At1g32770; Table II), two PC-biased G2-like genes

**Table II.** *Relative signal intensities and tissue biases for genes known or proposed for this report to have roles in vascular tissue differentiation or function*

| Locus | Gene Symbol | Description | $Log_2$ (X versus PC)[a] | $Log_2$ (X versus NV) | $Log_2$ (PC versus NV) | Tissue Bias, This Report[b] | Role in Vascular Tissue Differentiation[c] | Reference |
|---|---|---|---|---|---|---|---|---|
| At4g32880 | ATHB-8 | Homeobox-Leu zipper family | 2.6* | 4.4* | 1.8* | X | Vascular differentiation | Baima et al. (2001) |
| At1g30490 | ATHB-9/ PHV | Homeobox-Leu zipper family | 2.0* | 2.4* | 0.4 | X | Vascular bundle organization | McConnell et al. (2001) |
| At2g34710 | ATHB-14/ PHB | Homeobox-Leu zipper family | 1.7* | 2.9* | 1.3 | X | Vascular bundle organization | McConnell et al. (2001) |
| At1g52150 | ATHB-15 | Homeobox-Leu zipper family | 2.8* | 3.6* | 0.9 | X | ? | |
| At5g60690 | REV/IFL1 | Homeobox-Leu zipper family | 2.0* | 3.5* | 1.5 | X | Vascular patterning | Zhong and Ye (2004) |
| At1g02250 | ANAC005 | NAC domain | 2.3* | 2.5* | 0.3 | X | ? | |
| At1g32770 | ANAC012 | NAC domain | 4.5* | 3.6* | −0.8 | X | ? | |
| At2g46770 | ANAC043 | NAC domain | 3.4* | 2.6* | −0.8 | X | ? | |
| At4g28500 | ANAC073 | NAC domain | 2.3* | 5.1* | 2.8 | X | ? | |
| At4g28530 | ANAC074 | NAC domain | 1.9* | 1.6* | −0.3 | X | ? | |
| At5g64530 | XND1/ ANAC104 | NAC domain | 5.9* | 6.4* | 0.5 | X | ? | |
| At1g63910 | MYB103 | R2R3 MYB | 2.0* | 3.0* | 1.0 | X | ? | |
| At4g33450 | MYB69 | R2R3 MYB | 4.2* | 3.0* | −1.2 | X | ? | |
| At1g17950 | MYB52 | R2R3 MYB | 5.6* | 2.3* | −3.2* | X | ? | |
| At3g46130 | MYB48 | R2R3 MYB | 3.6* | 3.8* | 0.1 | X | ? | |
| At5g12870 | MYB46 | R2R3 MYB | 3.6* | 2.9* | −0.8 | X | ? | |
| At1g66230 | MYB20 | R2R3 MYB | 4.8* | 5.7* | 0.9 | X | ? | |
| At1g79430 | APL | G2-like transcription factor | −6.2* | −1.4 | 4.8* | PC | Vascular differentiation | Bonke et al. (2003) |
| At3g12730 | | G2-like transcription factor | −3.6* | −0.6 | 3.0* | PC | ? | |
| At5g18240 | MYR1 | G2-like transcription factor | −4.8* | −0.3 | 4.5* | PC | ? | |
| At4g37750 | ANT | AP2 domain transcription factor | −2.9* | −0.6 | 2.3* | PC | ? | |
| At1g75820 | CLV1 | CLAVATA1 receptor kinase | −3.6* | 1.0 | 4.5* | PC | ? | |
| At4g20270 | | CLV1-like receptor kinase | −2.8* | 0.8 | 3.6* | PC | ? | |
| At2g31085 | CLE6 | CLAVATA3/ ESR-related 6 | −3.6* | −0.2 | 3.4* | PC | ? | |
| At1g69970 | CLE26 | CLAVATA3/ ESR-related 26 | −4.6* | −0.8 | 3.9* | PC | ? | |
| At2g28810 | | Dof transcription factor | −3.6* | −1.1 | 2.5* | PC | ? | |
| At5g62940 | | Dof transcription factor | −2.9* | 0.3 | 3.2* | PC | ? | |
| At1g07640 | OBP2 | Dof transcription factor | −4.9* | −1.6 | 3.3* | PC | ? | Kang and Singh (2000) |
| At1g32240 | KAN2 | G2-like transcription factor | −4.2* | −3.9* | 0.2 | PC/NV | Vascular bundle organization | Emery et al. (2003) |
| At4g17695 | KAN3 | G2-like transcription factor | −3.6* | −3.2* | 0.4 | PC/NV | Vascular bundle organization | Emery et al. (2003) |
| At5g64080 | XYP1 | Lipid transfer protein (LTP) family protein | −1.9* | −1.8* | 0.1 | PC/NV | Vascular patterning | Motose et al. (2004) |
| At2g01830 | AHK4/WOL/ CRE1 | His kinase | 0.9 | 2.3* | 1.4 | NS | Vascular differentiation | Inoue et al. (2001); Mahonen et al. (2000); Scheres et al. (1995) |
| At1g20330 | CVP1 | *S*-Adenosyl-Met-sterol-C-methyltransferase | −1.3 | −0.8 | 0.5 | NS | Vascular patterning | Carland et al. (2002) |

(*Table continues on following page.*)

**Table II.** (*Continued from previous page.*)

| Locus | Gene Symbol | Description | $Log_2$ (X versus PC)[a] | $Log_2$ (X versus NV) | $Log_2$ (PC versus NV) | Tissue Bias, This Report[b] | Role in Vascular Tissue Differentiation[c] | Reference |
|---|---|---|---|---|---|---|---|---|
| At3g52940 | FK | C-14 sterol reductase | −0.7 | −0.4 | 0.3 | NS | Vascular patterning | Jang et al. (2000) |
| At1g13980 | GNOM/ EMB30 | Unclassified | −0.1 | −0.3 | −0.2 | NS | Vascular patterning | Steinmann et al. (1999) |
| At1g19850 | MP/IAA24 | IAA protein 24 | 0.4 | 1.7 | 1.3 | NS | Vascular differentiation | Hardtke and Berleth (1998) |
| At1g73590 | PIN1 | Auxin efflux carrier protein | 1.0 | 2.2* | 1.3 | NS | Vascular patterning | Galweiler et al. (1998) |

[a]$Log_2$ of the signal ratio for the three pair-wise tissue comparisons as described for Table I. $Log_2$ values representing pair-wise comparisons between significantly different signals are indicated by a single asterisk. [b]NS, Not significantly tissue biased in any pair-wise comparison or tissue biased in only one pair-wise comparison. Other abbreviations introduced in text. [c]Terms used to describe vascular tissue roles for characterized genes are from Ye (2002). ?, Genes identified for this report that may play roles in vascular tissue differentiation or function.

(At2g03500 and At3g04030; Supplemental Table I), and one major latex protein-related gene (At3g26450; Supplemental Table V) was performed using RNA isolated from X, PC, and NV tissues. The tissue-biased expression patterns and relative expression levels revealed for these five genes by 24 K GeneChip analysis (Supplemental Tables I, III, and V) were confirmed by RT-PCR (Fig. 5).

### Summary of Six Gene Sets from the Root-Hypocotyl

The members of six gene sets shown in Figure 3 have been tentatively placed into functional categories based on those used by the Munich Information Center for Protein Sequences (http://mips.gsf.de/proj/funcatDB/search_main_frame.html) and summarized in Table III. The detailed lists for all six gene sets can be found in the supplemental data section (Supplemental Tables III–VIII). The X gene set comprises the largest membership, 319, and is approximately 2-fold larger than the NV set, which, at 154 members, is the smallest one-tissue set. The PC and PC/NV sets are of similar size at 211 and 241, respectively. The X/PC and X/NV sets are very small (29 and 37 members, respectively). Not surprisingly, the X gene set includes the greatest number of genes in the ''biogenesis of cell wall'' and ''lignin biosynthesis'' categories. Together, these two categories include 56 genes, or 17% of the total X gene set. The membership of these two cell wall-related categories includes several examples of apparent redundancy, e.g. four chitinases, three arabinogalactans, four glycosyl hydrolases, three glycosyl transferases, four polygalacturonases, two lipid transfer proteins, two cinnamyl-alcohol dehydrogenases, five laccases, and eight peroxidases. This high level of potential redundancy is consistent with that found for several other gene families known or predicted to be involved in regulating vascular tissue development (discussed below). The PC sample is most active in the ''cell rescue, defense, cell death, and aging'' and ''cellular communication and signal transduction'' categories, which together account for 58 genes, or 27% of the PC set membership. Nonvascular tissue is most active in the ''cell rescue, defense, cell death, and aging'' and ''metabolism'' categories, i.e. 57 genes, accounting for 37% of the NV set membership.

### Previously Characterized Genes Involved in Vascular Tissue Development in Arabidopsis

In addition to the *APL* and *IRX* genes mentioned above (Table I), we considered the expression of other genes cloned from vascular tissue mutants and exhibiting MSIs >200 for at least one tissue. *AHK4/WOL/CRE1* (At2g01830; Scheres et al., 1995; Mahonen et al., 2000; Inoue et al., 2001), *CVP1* (At1g20330; Carland et al., 2002), *GNOM/EMB30* (At1g13980; Steinmann et al., 1999), *PIN1* (At1g73590; Galweiler et al., 1998), *FK* (At3g52940; Jang et al., 2000), and *MP/IAA24* (At1g19850; Hardtke and Berleth, 1998) were expressed in the root-hypocotyl, but did not exhibit the one- or two-tissue-biased expression patterns considered for this report (Table II). By contrast, *XYP1* (At5g64080; Motose et al., 2004) did exhibit a significant tissue-biased (PC/NV) expression pattern within the root-hypocotyl (Table II). This PC/NV-biased expression observed for *XYP1* contrasts with the leaf xylem localization reported for the putative orthologous Zinnia protein (Motose et al., 2004).

Several studies have led to the proposal that transcription factors REV/IFL1 (At5g60690), ATHB-14/PHB (At2g34710) and ATHB-9/PHV (At1g30490; class III HD-ZIP family), and KANADI homologs (KAN1, KAN2, KAN3, and KAN4, members of the G2-like subfamily of GARP transcription factors; Riechmann et al., 2000) serve complementary roles in the establishment and maintenance of leaf adaxial and abaxial identity. Radial patterning in stems that consist of central xylem and peripheral phloem and pericycle activity required for lateral root formation also depend on the *HD-ZIP/KANADI* genetic system (Talbert et al.,

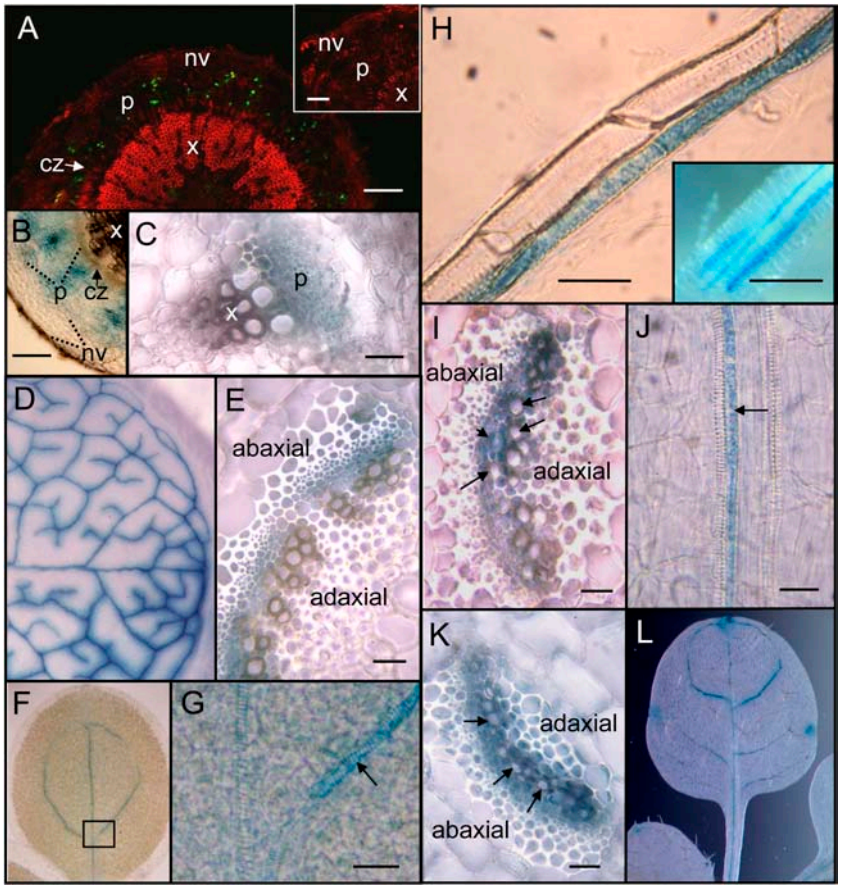


**Figure 4.** Promoters for *CLV1*, *MYR1*, *ZFWD1*, *XND1/ANAC104*, and *At1g20160* direct expression of reporters in vascular tissues as predicted from genome-wide transcript profiles of isolated vascular tissues. A, GFP expression driven by the promoter for *CLV1* localized to the cambial zone and secondary phloem. A, Inset, The secondary phloem of wild-type control plants exhibited no detectable green fluorescence. B and C, GUS activity driven by the promoter for the phloem-cambium-biased, G2-like transcription factor *MYR1* was detected in the secondary phloem of the root (B) and inflorescence stem (C). D and E, GUS activity due to the *MYR1* promoter was also detected throughout the vascular tissue of the leaf (D), where it localized predominantly to the abaxial (phloem) side of the vascular bundle, as shown in a transverse section through a midvein (E). F, GUS activity driven by the promoter for the xylem-biased gene *ZFWD1* was limited to vascular tissues. G, Higher magnification of the area within the black box (F) revealed that *ZFWD1p*::*GUS* expression was associated with xylem cells (arrow). H, *XND1/ANAC104* promoter-driven GUS activity visible beneath the bark of roots on 8-week-old plants (H, inset) was localized to xylem vessels, shown here following isolation of two adjacent vessels (one mature GUS-negative and one immature GUS-positive) from secondary xylem. I, *XND1p*::*GUS* expression in the shoot was limited to senescing leaves, where it was evident in xylem cells surrounding mature vessels (arrows) and immature vessels (arrowhead) in the midvein. J, *XND1p*::*GUS* expression in the primary tissues of seedling roots was limited to TEs, as shown for metaxylem cells (arrow) adjacent to mature protoxylem cells. K, GUS activity driven by the promoter for a xylem-biased subtilisin-like Ser protease At1g20160 was localized predominantly in xylem cells surrounding mature vessels (arrows) and additional cells on the adaxial (xylem) side of the midvein. L, Vascular tissue-localized expression for *At1g20160p*::*GUS* is shown in a representative leaf. A, The free-hand transverse section was prepared from a 6-week-old (or 5-week-old for inset) hypocotyl, and cell walls were counterstained with propidium iodide prior to detection of GFP by confocal microscopy. B, C, E, I, and K, Free-hand transverse sections of root-hypocotyl, stem, or petiole were prepared following histochemical staining for GUS activity. D, Whole-mount leaf from a 5-week-old plant. F and G, Whole-mount cotyledon from a 3-d-old seedling. H, Xylem vessels were isolated from a root similar to that shown in the inset following histochemical staining for GUS activity. J, Whole-mount root from a 3-d-old seedling. L, Whole-mount leaf from a 4-week-old plant. cz, Cambial zone; nv, nonvascular tissue; p, phloem; x, xylem. Bars = 100 $\mu$m (A, inset in A, and B); 50 $\mu$m (C); 25 $\mu$m (E, G, H, I, J, and K); 500 $\mu$m (inset in H). B, Broken lines indicate the limit of phloem or nonvascular tissues.

1995; Kerstetter et al., 2001; McConnell et al., 2001; Emery et al., 2003; Hawker and Bowman, 2004; Zhong and Ye, 2004). We found that *REV/IFL1*, *ATHB-14/PHB*, and *ATHB-9/PHV* as well as two related class III HD-ZIP genes, *ATHB-8* (At4g32880; Baima et al., 2001) and *ATHB-15* (At1g52150), all exhibited X-biased expression (Table II). Of the four *KAN* genes, *KAN1* (At5g16560) was scored as absent and *KAN4* (At5g42630) transcript was present at very low levels (MSIs <200) throughout the root-hypocotyl (Supplemental Tables I and II), while *KAN2* (At1g32240) and *KAN3* (At4g17695) expression patterns placed them in

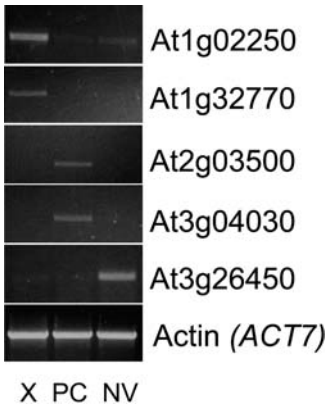


**Figure 5.** RT-PCR results for selected tissue-biased genes are consistent with predictions from genome-wide transcript profiles of isolated vascular tissues. Ethidium bromide-stained gels show products of RT-PCR for tissue-biased genes selected from xylem (X; At1g02250 and At1g32770), phloem-cambium (PC; At2g03500 and At3g04030), and nonvascular (NV; At3g26450) gene sets. Numbers of PCR cycles used were 27 for At3g26450 and actin (*ACT7*) and 30 for At1g02250, At1g32770, At2g03500, and At3g04030. Different PCR cycle numbers and annealing temperatures were evaluated before these representative experiments were selected for presentation.

the PC/NV gene set (Table II). The complementary expression domains observed for class III HD-ZIP genes and *KAN2* within secondary tissues of the root-hypocotyl are consistent with those reported for lateral roots (Hawker and Bowman, 2004), suggesting that these two classes of transcription factors maintain central versus peripheral identity in the root-hypocotyl through advanced stages of secondary growth.

### Hormone Metabolism, Transport, and Signal Transduction

Auxin and cytokinin are important regulators of xylem cell differentiation (Aloni, 1988; Ye, 2002; Fukuda, 2004). The PC and X/PC gene sets contain genes encoding cytokinin synthases (At3g63110 and At5g19040) previously reported to be associated with the phloem (Takei et al., 2004; Table IV). CYP79B3 (At2g22330) and CYP79B2 (At4g39950) catalyze the conversion of Trp to indole-3-acetaldoxime (IAOx; Hull et al., 2000), a key branching point between indole-3-acetic acid (IAA) and glucosinolate synthesis (Glawischnig et al., 2004 ). *CYP79B3* expression was PC biased (Table IV; *CYP79B2* was also PC biased but only to the $P = 0.01$ level and therefore was not included in the PC gene set). The nitrilases NIT1 (At3g44310) and NIT2 (At3g44300) that catalyze the final step in IAA synthesis via indole-3-acetonitrile and the cytochrome P450 CYP83B1 (At4g31500) that catalyzes the oxidation of IAOx for glucosinolate biosynthesis were expressed throughout the root-hypocotyl (Supplemental Table I). The PC-biased expression of *CYP79B3* suggests that the phloem is an important site for channeling Trp into auxin and/or glucosinolate biosynthesis. The putative auxin transporter *AUX1* (At2g38120; Timpte et al., 1995; Bennett et al., 1996) is a member of the X gene set (Table IV). Overexpression of the gibberellin (GA) biosynthetic enzyme GA 20-oxidase can promote xylem differentiation (Biemelt et al., 2004) and fiber elongation (Eriksson et al., 2000), while overexpression of the GA inactivator GA 2-oxidase can reduce xylem production (Biemelt et al., 2004). Although GA 20-oxidase (*GA5*/At4g25420) expression was not detected in the root-hypocotyl (Supplemental Table II), PC-

**Table III.** *Summary of the six root-hypocotyl gene sets organized by functional category*

Within each tissue-biased gene set, the percentage of genes in each functional category is shown followed by the number (in parentheses) of genes in each category. The single highest-ranking category (for xylem/phloem-cambium and xylem/nonvascular) or two highest-ranking categories (for xylem, phloem-cambium, nonvascular, and phloem-cambium/nonvascular) for each gene set, from among the classified genes, are shown in bold.

| Functional Category | Tissue-Biased Gene Set | | | | | |
|---|---|---|---|---|---|---|
| | Xylem | Phloem-Cambium | Nonvascular | Xylem/ Phloem-Cambium | Xylem/ Nonvascular | Phloem-Cambium/ Nonvascular |
| Biogenesis of cell wall | **11 (35)** | 9 (18) | 10 (16) | 0 | 5 (2) | **12 (28)** |
| Cell rescue, defense, cell death, and aging | 7 (24) | **13 (28)** | **17 (26)** | 14 (4) | **24 (9)** | 8 (20) |
| Cellular communication/signal transduction | **11 (34)** | **14 (30)** | 3 (4) | **35 (10)** | 3 (1) | 11 (26) |
| Cytoskeleton | <1 (1) | 0 | 0 | 0 | 0 | 0 |
| DNA/RNA binding | 0 | 0 | 3 (4) | 0 | 0 | <1 (1) |
| Energy | 2 (5) | 2 (4) | 1 (2) | 0 | 0 | 1 (3) |
| Lignin biosynthesis | 6 (21) | 1 (2) | 6 (10) | 0 | 5 (2) | 2 (5) |
| Metabolism | 9 (28) | 10 (21) | **20 (31)** | 10 (3) | 11 (4) | **19 (46)** |
| Protein destination | 0 | 0 | 0 | 0 | 0 | 0 |
| Proteolysis | 6 (18) | 5 (11) | 1 (2) | 3 (1) | 11 (4) | 6 (15) |
| Secondary metabolism | 4 (12) | 5 (11) | 5 (8) | 0 | 8 (3) | 3 (8) |
| Transcription | 10 (33) | 9 (18) | 8 (12) | 7 (2) | 5 (2) | 10 (24) |
| Transport facilitation | **11 (34)** | 7 (15) | 11 (17) | 17 (5) | 3 (1) | 10 (25) |
| Unclassified | 23 (74) | 25 (53) | 14 (22) | 14 (4) | 24 (9) | 17 (40) |
| Set total | (319) | (211) | (154) | (29) | (37) | (241) |

**Table IV.** *Relative signal intensities and tissue biases for selected genes involved in hormone metabolism or transport*

| Locus | Gene Symbol | Description | $Log_2$ (X versus PC)[a] | $Log_2$ (X versus NV) | $Log_2$ (PC versus NV) | Tissue Bias, This Report[b] | Role in Hormone Metabolism/Transport | Reference |
|---|---|---|---|---|---|---|---|---|
| At2g38120 | AUX1 | Amino acid/auxin permease | 1.5* | 2.0* | 0.6 | X | Auxin transport | Bennett et al. (1996) |
| At1g30040 | GA2OX2 | GA 2-oxidase | 3.6* | 4.6* | 1.1 | X | Gibberellic acid inactivation | |
| At2g22330 | CYP79B3 | Cytochrome P450, converts Trp to IAOx | −3.3* | −0.9 | 2.4* | PC | Auxin biosynthesis | Hull et al. (2000) |
| At1g15550 | GA4 | GA 3-$\beta$-dioxygenase/ GA 3-$\beta$-hydroxylase | −3.5* | 0.8 | 4.4* | PC | Gibberellic acid biosynthesis | Williams et al. (1998) |
| At5g19040 | IPT5 | Adenylate isopentenyl-transferase 5/cytokinin synthase | −6.0* | −2.2 | 3.9* | PC | Cytokinin biosynthesis | Takei et al. (2004) |
| At3g63110 | IPT3 | Adenylate isopentenyl-transferase 3/cytokinin synthase | −1.2 | 2.0* | 3.2* | X/PC | Cytokinin biosynthesis | Takei et al. (2004) |

[a]$Log_2$ of the signal ratio for the three pair-wise tissue comparisons as described for Table I. $Log_2$ values representing pair-wise comparisons between significantly different signals are indicated by a single asterisk. [b]Abbreviations for tissue biases are as described for Tables I and II.

biased expression was noted for GA 3-$\beta$-hydroxylase (*GA4*/At1g15550), which catalyzes the last step in the formation of active GAs (Williams et al., 1998; Table IV). The magnitude of any GA-mediated effects on xylem cell expansion or differentiation may be governed by the X-biased GA 2-oxidase *GA2OX2* (At1g30040; Table IV).

### Regulatory Genes with Possible Roles in Vascular Tissue Development or Function

G2-like, Dof, and NAC proteins are three examples of plant-specific transcription factors (Riechmann et al., 2000) that are well represented in the X and PC gene sets and may perform vascular tissue-specific functions. The PC-biased gene *APL*, like *KAN*, is a member of the G2-like family of transcription factors. *APL* is joined in the PC-biased gene set by two uncharacterized G2-like genes, *MYR1* and At3g12730 (Table II). Two additional PC-biased G2-like genes, At3g04030 and At2g03500, were not included in the PC set, as their MSIs were below 200 (Supplemental Table I). We noted three PC-biased Dof genes, including the auxin- and salicylic acid-responsive gene *OBP2* (At1g07640; Kang and Singh, 2000). *OBP3* (At3g55370), an additional PC-biased Dof gene, was not included in the PC set, as its MSI was below 200 (Supplemental Table I). Notably, a reported target of OBP3, the bHLH transcription factor gene *ORG3* (At3g56980; Kang et al., 2003), was also a PC-biased gene (Supplemental Table IV). A recent effort to silence *OBP3* expression did not yield any obvious phenotype (Kang et al., 2003). Perhaps *OBP3* is redundant with *OBP2* and other PC-biased Dofs identified for this report. Although NAC transcription factors have not yet been directly linked to vascular tissue development, we noted that six uncharacterized NAC-domain genes (discussed below) were X biased (Table II).

We found that *CLV1* was expressed in the phloem and cambium (Table II; Fig. 4A). In the shoot apical meristem, CLV1 probably forms a heterodimer with the receptor-like protein CLV2 (At1g65380; Jeong et al., 1999) and binds a ligand encoded by the CLE-family gene, *CLV3* (At2g27250). *CLV2* was expressed at low levels throughout the root-hypocotyl, i.e. it was not significantly tissue biased, and *CLV3* was scored as absent from all root-hypocotyl tissues (Supplemental Table I). However, an uncharacterized *CLV1*-like gene, At4g20270, and two uncharacterized CLE-family members, *CLE26* (At1g69970) and *CLE6* (At2g31085), were PC biased (Table II). CLAVATA-based meristem maintenance is integrated with activity of the homeobox family gene *WUS* (At2g17950; Schoof et al., 2000). However, *WUS* was scored as absent from all tissues of the root-hypocotyl (Supplemental Table II). The G2-like, NAC, Dof, CLV-like, and CLE genes are but a few examples of potential regulators of vascular tissue differentiation and function. Additional regulatory genes listed among the X and PC genes include, for example, many Leu-rich repeat transmembrane protein kinases, protein phosphatases, ubiquitin E3 ligases, and transcription factors belonging to the MYB, MADS, bZIP, WRKY, and bHLH families (Supplemental Tables III and IV).

## DISCUSSION

Here, we present genome-wide expression profiles from isolated xylem and phloem-cambium. An analysis of the distribution of transcripts for previously published markers for TEs, SEs, and/or CCs and nonvascular root peripheral tissue indicated that the X and PC samples contained very low to nondetectable (i.e. scored as absent; Supplemental Table II) levels of contamination from adjacent tissues (Table

I; Supplemental Fig. 1). Although the tissues used for this study contained no apical meristems, we found that a known apical meristem marker (*CLV1*; Clark et al., 1997) and a cell proliferation marker (*ANT*; Mizukami and Fischer, 2000) were associated with the PC sample, indicative of the presence of meristematic cells in the PC sample. Tissue-biased genes were identified and assembled into three one-tissue and three two-tissue gene sets to be used for identification of new genes with potential roles in vascular tissue differentiation and function. Results from promoter-reporter and RT-PCR experiments for nine genes not previously localized to xylem or phloem-cambium faithfully reflected localizations predicted by 24 K GeneChip transcript profiling of isolated secondary tissues.

### Secondary Tissue Gene Sets Are Tools for Studying Specialized Metabolism in Vascular Conducting and Nonconducting Cells and the Outer Bark

Secondary tissue expression profiles revealed novel restricted expression patterns for genes known or predicted to be required for glucosinolate, suberin, and lignin biosynthesis. Glucosinolates accumulate in the phloem cells adjacent to SEs (Koroleva et al., 2000). In Arabidopsis, specialized phloem idioblasts containing myrosinase and adjacent glucosinolate-rich S-cells are thought to comprise a two-component system of defense against herbivory (Husebye et al., 2002). Our results implicate the phloem-cambium as the root-hypocotyl tissue most active in channeling Trp to IAOx, the common precursor for auxin and indole glucosinolate biosynthesis (discussed above). We also found that *MAM1* (At5g23010) was a PC-biased gene (Supplemental Table IV). MAM1 catalyzes the initial reactions of chain elongation of the 2-oxo-acid Met derivatives leading to the biosynthesis of the predominant glucosinolate (Kroymann et al., 2001). Importantly, CYP83A1 (At4g13770), the cytochrome P450 capable of metabolizing the oxime derivatives of chain-elongated Met homologs (Naur et al., 2003), was also PC biased (Supplemental Table IV). This localization of *MAM1* and *CYP83A1* transcripts highlights the value of the PC gene set as a resource for novel discoveries regarding important processes localized in phloem cells. We found that KCS1 (At1g01120), a fatty acid elongase 3-ketoacyl-CoA synthase required for the C26 and C30 wax alcohol and aldehyde components of epicuticular waxes and/or suberin (Todd et al., 1999), was an NV-biased gene (although *KCS1* signal was below the 200 MSI cutoff; Supplemental Table I), perhaps reflecting a role for KCS1 in suberization of cork cells (Chaffey et al., 2002). In addition, membership in the X/NV set (Supplemental Table VII) for two lignin biosynthesis genes, cinnamoyl-CoA reductase (At1g80820) and *O*-methyltransferase (At1g21100), suggests that some lignin pathway genes serve dual roles in defense/wound responses and xylem secondary cell wall lignification. *MYB46* (At5g12870) and *MYB52* (At1g17950) were among the X-biased R2R3 MYB genes (Table II). *MYB46* is a predicted ortholog of *PtMYB4*, a positive regulator of lignification of xylem cells and phloem fibers in loblolly pine (Patzlaff et al., 2003). *MYB52* is a predicted ortholog of the X-biased poplar MYB *PttMYB21a*, a proposed transcriptional repressor of caffeoyl-CoA 3-*O*-methyltransferase gene expression (Karpinska et al., 2004). Thus, Arabidopsis X gene set membership for *MYB46* and *MYB52* is consistent with previous predictions of orthology to X-biased MYBs from pine and poplar, respectively. Reverse genetic experiments in Arabidopsis using *MYB46* and *MYB52* and other X-biased MYBs can form the basis of a relatively rapid assessment of MYB gene regulation of lignification in vascular tissues.

### Arabidopsis Secondary Tissue Is a Good Model for Studying Transitions from Cell Division to Cell Expansion to Cell Differentiation

Lateral expansion of organs due to the growth of secondary vascular tissues occurs as a result of extended periods of cambial cell division that produce a zone of meristematic cells, the cambial zone. These cambial derivatives expand and eventually differentiate to yield the various xylem and phloem cell types. For the secondary phloem to keep pace with the increase in circumference driven by the vascular cambium, localized dilations and/or divisions of ray or axial phloem parenchyma cells occur (Esau, 1965). *CLV1p*::*GFP* expression was not detected uniformly throughout the cambium and phloem, suggesting cell type-specific localization for CLV1 in secondary phloem. Perhaps *CLV1* restricts the size of the zones of dilating or dividing phloem parenchyma cells as well as phloem-side cambium cell activity, similar to its role in restricting the size of the pool of undifferentiated cells in the shoot and flower apical meristems (Carles and Fletcher, 2003). As we observed low or absent expression of *CLV2*, *CLV3*, and *WUS*, an alternative to the apical meristem CLV-WUS signaling system is probably active in secondary tissues. Candidate *CLV1*-like and CLE-family genes that could interact with CLV1 in the phloem-cambium are evident among the PC-biased genes (Table II) and provide a starting point for reverse genetics of CLV1-based signaling in the phloem and cambium. Absence of *CLV3* and *WUS* transcripts from secondary tissues of Arabidopsis is consistent with the absence of *PttCLV3* and *PttWUS* transcripts from the cambium of aspen (Schrader et al., 2004). In secondary vascular tissues of Arabidopsis and many other species, more xylem is produced than phloem. Through both loss-of-function (Elliott et al., 1996; Klucher et al., 1996) and gain-of-function (Mizukami and Fischer, 2000) experiments, it has been shown that *ANT* regulates organ growth through the maintenance of meristematic activity. *ANT* may act as a regulator of this common vascular asymmetry by prolonging the period of proliferation

(Mizukami and Fischer, 2000) of xylem mother cells relative to that of phloem mother cells.

Expansins can induce extension of cell walls (for review, see Darley et al., 2001; Cosgrove et al., 2002). The tentative conclusion that radially expanding xylem cells partitioned with the PC sample is based on the PC-biased expression of *EXPA9*, a subfamily A $\alpha$-expansin homologous to *PttEXP1*, recently localized to radially expanding xylem and cambium cells of aspen (Gray-Mitsumune et al., 2004). Other subgroup A $\alpha$-expansins, *EXPA4* (At2g39700) and *EXPA6* (At2g28950), were expressed in the root-hypocotyl but did not exhibit significant tissue-biased expression (Supplemental Table I). Subgroup A $\alpha$-expansins *EXPA3* (At2g37640) and *EXPA16* (At3g55500) were scored as absent from all tissues of the root-hypocotyl (Supplemental Table II). The expression patterns observed for subgroup A $\alpha$-expansins in Arabidopsis secondary tissues point to roles for *EXPA4*, *EXPA6*, and *EXPA9*, with the latter being the best candidate for a cambial zone/radially expanding xylem gene. Our findings for expansins expand on those reported by Gray-Mitsumune et al. (2004), who also found *EXPA4*, *EXPA6*, and *EXPA9* to be expressed in hypocotyls but did not report tissue-level localization of expansin transcripts in Arabidopsis.

A consideration of the predicted transcription factors belonging to the PC and PC/NV gene sets reinforces the importance of known G2-like genes, *KAN* and *APL*, to the regulation of peripheral cell identity and patterning and predicts that other G2-like genes are important to phloem differentiation (Table II). Although loss of function for *APL* alone was sufficient to block SE differentiation and allow ectopic TE differentiation in the stele of Arabidopsis seedlings, *APL* overexpression did not lead to ectopic phloem formation (Bonke et al., 2003). Hence, there is still much to learn about the requirements for phloem cell identity. Studies with the uncharacterized G2-like genes shown here to exhibit restricted expression patterns in secondary tissues may help to refine our current understanding of the control of radial patterning and phloem cell fate in plants.

Members of the NAC family of transcription factors may figure prominently in transitions across developmental boundaries relevant to late stages of xylem development. NAC proteins are involved in maintaining organ or tissue boundaries (Souer et al., 1996; Takada et al., 2001; Vroemen et al., 2003; Weir et al., 2004), regulating the transition from growth by cell division to growth by cell expansion (Sablowski and Meyerowitz, 1998) and promoting lateral root development (Xie et al., 2000). Several NAC genes are also up-regulated during leaf senescence in Arabidopsis (Guo et al., 2004) and following stress (Tran et al., 2004). We have identified six NAC genes as members of the X gene set (Table II). An embryo-lethal, globular-stage phenotype results from a mutation of one of the X-biased NAC-domain genes (At2g46770), as reported by the SeedGenes project (http://www.seedgenes.org). Another X-biased NAC gene, *XND1/ANAC104*, was identified as part of the leaf senescence transcriptome (Guo et al., 2004). Overexpression of *XND1* in Arabidopsis blocks TE differentiation, as indicated by the absence of patterned secondary cell walls, lack of expression of xylem markers *XSP1p*::*GUS* and *XCP2p*::*GUS*, and failure of cells in vascular bundles to undergo programmed cell death (C. Zhao and E. Beers, unpublished data). These preliminary findings and the current understanding of NAC family gene functions suggest that xylem differentiation is another aspect of plant development that depends on NAC gene activity.

### Repeatability and Limitations of Tissue-Biased Gene Sets

Using isolated xylem and bark for gene expression profiling via the 8 K GeneChip, Oh et al. (2003) assembled a 304-member xylem gene set. The number of genes shared between the 304-gene set from the 8 K GeneChip (Oh et al., 2003) and the 319-gene set from the 24 K GeneChip (this report) is 79 (26% of 304). Excluding from the comparison the 204 genes reported by Oh et al. (2003) to exhibit a xylem/bark signal ratio $\leq$4 increased X set identity between the two experiments to 58% (58 out of 100). Further exclusion of the 266 genes exhibiting a xylem/bark signal ratio $\leq$9 increased the level of genes shared by the X sets from both experiments to 68% (26 out of 38). As the 8 K GeneChip interrogated only 103 of the 319 X-set members identified for this report, a higher level of identity between independently generated gene sets would probably be achieved using the same 24 K GeneChips. Nevertheless, the results of this comparison suggest that the initial selection of X or PC genes for functional analysis should focus on those with between-tissue expression ratios $\geq$10 ($\log_2$ of 10 is approximately 3.3). More than 40% of the genes in the X and PC gene sets are above this 10-fold-difference level. In a recently published comparison of transcription factor transcripts detected by the 24 K GeneChip versus measurement by real-time RT-PCR, good correlation was found for highly expressed genes, while the opposite was true for genes expressed at low levels, as many of these were incorrectly scored as absent by GeneChip analysis (Czechowski et al., 2004). Indeed, our own analysis, by RT-PCR, of four minimally expressed X- and PC-biased genes and one highly expressed NV-biased gene (all of which were scored as absent from adjacent tissues) revealed that, while the original tissue-bias designations were upheld, cDNA from two of the five genes (At1g02250 and At3g26450) was detectable at very low levels in samples from adjacent tissue (Fig. 5) and was therefore incorrectly scored as absent (Supplemental Table II). Hence, consideration should be given to reanalyzing, e.g. by semiquantitative or real-time RT-PCR, selected genes scored as absent in GeneChip analyses. Such analyses may be important, for example, for identify-

ing all coexpressed, potentially redundant members of multigene families for the preparation of effective multigene loss-of-function lines.

## CONCLUSION

The X and PC gene sets assembled for this report are valuable resources for predicting new genes that are potential regulators of vascular tissue development and function. The gene sets also reveal the identity of coexpressed members of large multigene families that can be considered in the rational design of multigene knockout lines for functional analysis. Examples of candidate regulatory genes identified for this report include uncharacterized G2-like and class III HD-ZIP genes, homologous to genes already linked with vascular tissue development, as well as NAC, MYB, MADS box, bHLH, or WRKY genes, for which roles in vascular cell differentiation have not yet been established. Regulation of the vascular cambium, and perhaps of dilating or dividing phloem cells, may require the activity of CLV1 and ANT, two regulators of meristematic activity not previously reported to be linked with Arabidopsis secondary tissues. The gene sets reported here also include potential participants in secondary metabolic pathways that contribute to the structural and functional features unique to vascular tissues. The availability of these genome-wide xylem and phloem-cambium expression profiles from Arabidopsis should rapidly lead to new discoveries that enhance our understanding of vascular cell differentiation and function. Given the high degrees of anatomical (Chaffey et al., 2002) and genomic (Kirst et al., 2003) similarities regarding wood formation in Arabidopsis compared with that in poplar (Chaffey et al., 2002) and loblolly pine (Kirst et al., 2003), discoveries connected with these transcript profiles are also likely to lead to important applications in economically important trees species.

## MATERIALS AND METHODS

### Plant Material

Arabidopsis (*Arabidopsis thaliana* ecotype Col-0) was grown as described previously (Lev-Yadun, 1994; Zhao et al., 2000). On two separate harvest dates, >100 root-hypocotyl segments, 1 cm in length, beginning just below the cotyledons, were harvested from 8-week-old plants and dissected to isolate, in the following order, NV, PC, and X tissues (Zhao et al., 2000).

### Sample Preparation and Experimental Design

Total RNA, 15 $\mu$g isolated by RNeasy plant mini kit (Qiagen, Valencia, CA) from X, PC, and NV tissues, was used for the synthesis of biotin-labeled cRNA. Fragmented cRNA (15 $\mu$g) was used for hybridization according to the Affymetrix GeneChip (Affymetrix, Santa Clara, CA) expression analysis manual. Image acquisition and global data scaling were performed with the Affymetrix Microarray Suite version 5.0 (MAS 5.0; Affymetrix). Scaling factors for all arrays were within acceptable limits, as were background and mean intensities. Using X, PC, and NV tissues isolated from the root-hypocotyl, a total of nine hybridizations were performed: six hybridizations for technical duplicates (IA and IB) of the three tissues for biological replicate I plus three hybridizations, one for each tissue, for biological replicate II. The technical duplicates were performed using two aliquots of cRNA produced from the same cDNA amplification reaction.

### Data Preprocessing and Statistical Analysis

Affymetrix chip data was normalized using the MAS 5.0 software. The signal values from each chip were then scaled to a mean of 500. Within each tissue, the signal intensities for each gene from the three chips for each tissue sample (IA, IB, and II, with IA and IB being technical replicates) were combined into a MSI using the formula: MSI = {[(IA + IB)/2] + II}/2. Between-tissue correlations were performed using the ''cor'' function of the R statistical package (R Development Core Team, 2004; http://www.R-project.org). ANOVA was performed using the ''lm'' function of R with the model specified as ''signal approximately gene*tissue + rna%in%tissue + chip%in%rna.'' ANOVA was applied to five different samples consisting of every 20th gene, about 1,120 genes per sample.

Significance testing of the differences in mRNA levels between tissues for a single gene requires an estimate of the error variance. As is typical in microarray studies, our sample sizes were not large enough to reliably use the measured error variance for each gene independently, and the alternative of pooling variance across all genes is inappropriate because of the relationship between variability and mean expression level (Quackenbush, 2002). We pooled genes with some sensitivity to the signal intensity by dividing independent biological replicate pairs ($n$ = 67,434) into 50 equally spaced bins on the $\log_{10}$ (MSI) scale and calculated the SD of $\log_2$ (ratio) within each bin, similar to the approach of Quackenbush (2002). The SD of log ratios of biological replicates within each bin was used to calculate $Z$-scores of $\log_2$ (ratio) of between-tissue comparisons for the appropriate $\log_{10}$ (MSI) bin. This $Z$-score is expected to be slightly conservative because the error variance is estimated from ratios of single biological replicates while the between-tissue comparisons are ratios of means.

The ''triangle plot'' (Fig. 3) reduced three-valued expression points (A, B, C) to two dimensions by plotting A/2 + B versus A/(A + B + C). Location in the plot is based on proportionality among expression levels, ignoring magnitude. Genes whose expression is high in one tissue and low in the other two lie near a specific corner of the triangle, genes that are high in two tissues and low in the third are plotted along one edge of the triangle, and genes that are roughly equally expressed in all tissues fall toward the center. To reduce noise, we showed only genes with a minimum expression level of 200 in at least one tissue. We used larger dots to highlight genes with at least one significant pairwise $Z$-score ($P \leq 0.001$), red to highlight genes that were significantly higher in one tissue than both others (one-tissue genes), and green to highlight genes with similar expression in two tissues, both significantly higher than in the third tissue (two-tissue genes). The Java program implementing this visualization is available from A. Dickerman.

### Construction of Binary Vectors for Promoter-Reporter Experiments

#### *Modified pBI121 (mpBI121)*

To make the binary vector pBI121 (Jefferson et al., 1987) more convenient for cloning and the transgenic seedlings more easily selected, the *Bar* cassette and a polycloning site containing *Sma*I, *Pac*I, *Xba*I, *Avr*II, and *Bam*HI were inserted into the *Eco*RI and *Hin*dIII-*Bam*HI sites of pBI121, respectively.

#### *mpBI121-XND1p::GUS, mpBI121-MYR1p::GUS, mpBI121-ZFWD1p::GUS, and mpBI121-At1g20160p::GUS*

The putative promoters of *XND1*, *MYR1*, *ZFWD1*, and *At1g20160* (*XND1p*, *MYR1p*, *ZFWD1p*, and *At1g20160p*), 1.1-, 1.47-, 0.99-, and 1.08-kb regions upstream from the XND1, MYR1, ZFWD1, and At1g20160 translation start sites, respectively, were amplified from genomic DNA by PCR using the following primers: for *XND1p*, an upstream primer 5′-ACGATATCAAAAACGTTATTTTCAAA-3′, and a downstream *Bam*HI (underlined) linker primer 5′-GGATCCTGCTAACGATATTGATCTCACT-3′; for *MYR1p*, an upstream *Eco*RV linker primer 5′-GATATCAATTGCACATAGAGAAGCCA-3′ and a downstream *Bam*HI linker primer 5′-GGATCCAGTCTGTCTTCAAAATAAAAGG-3′; for *ZFWD1p*, an upstream *Hin*dIII linker primer 5′-AAGCTTAGAAACATTATGAGCTACATG-3′ and a downstream *Bam*HI linker

primer 5′-GGATCCCGAATTGGATTCTCTCTAAATT-3′; and for *At1g20160p*, an upstream *Hin*dIII linker primer 5′-AAGCTTAAGATACAAAGCACA-CCC-3′ and a downstream *Bam*HI linker primer 5′-GGATCCGGCTTTG-TAGTTTCCTAATC-3′. The resulting PCR products were cloned into the pGEM-T Easy vector (Promega, Madison, WI), thus producing pGEM-*XND1p*, pGEM-*MYR1p*, pGEM-*ZFWD1p*, and pGEM-*At1g20160p*. Plasmid DNA pGEM-*XND1p* and pGEM-*MYR1p* (antisense orientation) were digested with *Spe*I/*Bam*HI (the *Spe*I site is located on the vector), and the released fragments were ligated with mpBI121 previously digested with *Xba*I/*Bam*HI, thus generating mpBI121-*XND1p*::*GUS* and mpBI121-*MYR1p*::*GUS*, respectively. Plasmid DNA pGEM-*At1g20160p* and pGEM-*ZFWD1p* were digested by *Hin*dIII/*Bam*HI, and the released fragment was ligated with mpBI121 digested with *Hin*dIII/*Bam*HI, thus generating mpBI121-*At1g20160p*::*GUS* and mpBI121-*ZFWD1p*::*GUS*, respectively.

### *CLV1p::GFP*

Seeds for Arabidopsis (L*er*-0) transformed for expression of GFP driven by the *CLV1* promoter were provided by R. Sablowski (John Innes Centre, Norwich, UK). The *CLV1p*::*GFP* expression cassette is described by Gallois et al. (2002).

## RT-PCR

Total RNA was isolated from X, PC, and NV tissues by RNeasy plant mini kit (Qiagen). RT-PCR was carried out according to the RETROscript kit instruction manual (Ambion, Austin, TX), i.e. cDNA was synthesized from 1 $\mu$g of total RNA in 20-$\mu$L reaction. One microliter of cDNA was used as template for PCR amplification in a 25-$\mu$L reaction using the following pairs of primers (with one primer spanning a splice site for all templates except actin): for At1g02250, 5′-TTGGGACTTACCTTCCCATT-3′ and 5′-GTGAAAGAAA-CCAGCTCTTTTG-3′; for At1g32770, 5′-CCTTGGGATATTCAAGAGGA-3′ and 5′- GAAGTGGGTCTAAAGACGAA-3′; for At2g03500, 5′-CCTTAA-CAATGCTGTGGAAG-3′ and 5′-TCTTCCCTAAGAGCAGCCAA-3′; for At3g04030, 5′-TCATCTTCAGAAATACAGGCT-3′ and a *Sma*I linker primer 5′-CCCGGGAAACTCTCTTTTAACTTTTTGG-3′; for At3g26450, 5′-ACTA-CACACTCGGAGATGGA-3′ and 5′-TTAAGCTTTAAGGACGTGGTC-3; for actin (*ACT7*), 5′-GGCCGATGGTGAGGATATTC-3′ and 5′-CTGACTCATCG-TACTCACTC-3′.

## Histochemical Staining

Histochemical analysis of GUS expression was performed according to Oono et al. (1998). Tissues were vacuum infiltrated and incubated in staining buffer (100 mM sodium phosphate, pH 7.0, 10 mM EDTA, 0.5 mM $K_4Fe[CN]_6$, 0.5 mM $K_3Fe[CN]_6$, 0.1% Triton X-100, 1 mM 5-bromo-4-chloro-3-indolyl-$\beta$-D-glucuronide) for 2 to 18 h at 37°C. Chlorophyll was removed from stained tissues by incubating in 70% ethanol. Propidium iodide was used for counterstaining of cell walls for enhanced localization of GFP in *CLV1p*::*GFP* plants according to Haseloff et al. (1999). Hypocotyls were harvested, rinsed with double-distilled water, and sectioned with a double-edge razor blade. Transverse sections were incubated for 10 min at room temperature in 10 $\mu$g of propidium iodide/mL aqueous solution just prior to mounting in water for confocal microscopy. To visualize secondary versus primary cell walls in X, phloem, and NV tissues, transverse sections of fresh hypocotyl tissue were stained with toluidine blue O (TBO) and ruthenium red according to Chaffey et al. (2002).

## Microscopy

Photomicroscopy of GUS-expressing plants and the TBO/ruthenium red-stained hypocotyl sections was conducted using a Zeiss compound light microscope (Carl Zeiss, Thornwood, NY) and Ektachrome 160T slide film (Kodak, Rochester, NY). Slides were scanned and converted to digital images using a Minolta DiMAGE scan dual III slide scanner (Konica Minolta Photo Imaging, Mahwah, NJ). For GFP detection, imaging was performed using a Zeiss LSM 510 laser-scanning confocal microscope (software version 3.2) with a Zeiss Plan-Neofluar 10×, 0.3 numerical aperture. objective lens. GFP was visualized using the 488-nm argon laser line and a BP505-550 emission filter. Propidium iodide-stained cell walls were visualized using a 543-nm helium-neon laser line and a LP560 emission filter. The 488-nm and 543-nm channels were scanned consecutively.

## ACKNOWLEDGMENTS

We thank Dr. R. Evert for providing the translation of the Russian-language article by Kondratieva-Melville and Vodolazsky (1982), Dr. K. Decourcy for technical assistance with confocal microscopy, Dr. Susan Martino-Catt and the staff of the Virginia Bioinformatics Institute Core Laboratory for performing Affymetrix GeneChip hybridizations, Dr. R. Sablowski for providing seeds for the *CLV1p*::*GFP* plants, and Drs. T. Nelson and J. Tokuhisa for critical reading of the manuscript.

Received January 26, 2005; revised April 12, 2005; accepted April 13, 2005; published May 27, 2005.

## LITERATURE CITED

**Allona I, Quinn M, Shoop E, Swope K, St Cyr SS, Carlis J, Riedl J, Retzel E, Campbell MM, Sederoff R, et al** (1998) Analysis of xylem formation in pine by cDNA sequencing. Proc Natl Acad Sci USA **95:** 9693–9698

**Aloni R** (1988) Vascular differentiation within the plant. *In* LW Roberts, PB Gahan, R Aloni, eds, Vascular Differentiation and Plant Growth Regulators. Springer-Verlag, New York, pp 39–62

**An HL, Roussot C, Suarez-Lopez P, Corbesler L, Vincent C, Pineiro M, Hepworth S, Mouradov A, Justin S, Turnbull C, et al** (2004) CONSTANS acts in the phloem to regulate a systemic signal that induces photoperiodic flowering of Arabidopsis. Development **131:** 3615–3626

**Baima S, Possenti M, Matteucci A, Wisman E, Altamura MM, Ruberti I, Morelli G** (2001) The Arabidopsis ATHB-8 HD-zip protein acts as a differentiation-promoting transcription factor of the vascular meristems. Plant Physiol **126:** 643–655

**Beers EP, Jones AM, Dickerman AW** (2004) The S8 serine, C1A cysteine and Al aspartic protease families in Arabidopsis. Phytochemistry **65:** 43–58

**Bennett MJ, Marchant A, Green HG, May ST, Ward SP, Millner PA, Walker AR, Schulz B, Feldmann KA** (1996) Arabidopsis AUX1 gene: a permease-like regulator of root gravitropism. Science **273:** 948–950

**Biemelt S, Tschiersch H, Sonnewald U** (2004) Impact of altered gibberellin metabolism on biomass accumulation, lignin biosynthesis, and photosynthesis in transgenic tobacco plants. Plant Physiol **135:** 254–265

**Birnbaum K, Shasha DE, Wang JY, Jung JW, Lambert GM, Galbraith DW, Benfey PN** (2003) A gene expression map of the Arabidopsis root. Science **302:** 1956–1960

**Bonke M, Thitamadee S, Mahonen AP, Hauser MT, Herarlutta Y** (2003) APL regulates vascular tissue identity in Arabidopsis. Nature **426:** 181–186

**Busse JS, Evert RF** (1999) Pattern of differentiation of the first vascular elements in the embryo and seedling of Arabidopsis thaliana. Int J Plant Sci **160:** 1–13

**Carland FM, Fujioka S, Takatsuto S, Yoshida S, Nelson T** (2002) The identification of CVP1 reveals a role for sterols in vascular patterning. Plant Cell **14:** 2045–2058

**Carland FM, Nelson T** (2004) Cotyledon vascular pattern2-mediated inositol (1,4,5) triphosphate signal transduction is essential for closed venation patterns of Arabidopsis foliar organs. Plant Cell **16:** 1263–1275

**Carles CC, Fletcher JC** (2003) Shoot apical meristem maintenance: the art of a dynamic balance. Trends Plant Sci **8:** 394–401

**Chaffey N, Cholewa E, Regan S, Sundberg B** (2002) Secondary xylem development in Arabidopsis: a model for wood formation. Physiol Plant **114:** 594–600

**Chisholm ST, Parra MA, Anderberg RJ, Carrington JC** (2001) Arabidopsis *RTM1* and *RTM2* genes function in phloem to restrict long-distance movement of tobacco etch virus. Plant Physiol **127:** 1667–1675

**Clark SE, Williams RW, Meyerowitz EM** (1997) The CLAVATA1 gene encodes a putative receptor kinase that controls shoot and floral meristem size in Arabidopsis. Cell **89:** 575–585

**Clay NK, Nelson T** (2002) VH1, a provascular cell-specific receptor kinase that influences leaf cell patterns in Arabidopsis. Plant Cell **14:** 2707–2722

**Cosgrove DJ, Li LC, Cho HT, Hoffmann-Benning S, Moore RC, Blecker D** (2002) The growing world of expansins. Plant Cell Physiol **43:** 1436–1444

**Czechowski T, Bari RP, Stitt M, Scheible WR, Udvardi MK** (2004) Real-time RT-PCR profiling of over 1400 Arabidopsis transcription factors: unprecedented sensitivity reveals novel root- and shoot-specific genes. Plant J **38:** 366–379

**Darley CP, Forrester AM, McQueen-Mason SJ** (2001) The molecular basis of plant cell wall extension. Plant Mol Biol **47:** 179–195

**Demura T, Tashiro G, Horiguchi G, Kishimoto N, Kubo M, Matsuoka N, Minami A, Nagata-Hiwatashi M, Nakamura K, Okamura Y, et al** (2002) Visualization by comprehensive microarray analysis of gene expression programs during transdifferentiation of mesophyll cells into xylem cells. Proc Natl Acad Sci USA **99:** 15794–15799

**DeWitt ND, Sussman MR** (1995) Immunocytological localization of an epitope-tagged plasma membrane proton pump (H(+)-ATPase) in phloem companion cells. Plant Cell **7:** 2053–2067

**Dolan L, Roberts K** (1995) Secondary thickening in roots of Arabidopsis thaliana—anatomy and cell-surface changes. New Phytol **131:** 121–128

**Elliott RC, Betzner AS, Huttner E, Oakes MP, Tucker WQJ, Gerentes D, Perez P, Smyth DR** (1996) AINTEGUMENTA, an APETALA2-like gene of Arabidopsis with pleiotropic roles in ovule development and floral organ growth. Plant Cell **8:** 155–168

**Emery JF, Floyd SK, Alvarez J, Eshed Y, Hawker NP, Izhaki A, Baum SF, Bowman JL** (2003) Radial patterning of Arabidopsis shoots by class III HD-ZIP and KANADI genes. Curr Biol **13:** 1768–1774

**Eriksson ME, Israelsson M, Olsson O, Moritz T** (2000) Increased gibberellin biosynthesis in transgenic trees promotes growth, biomass production and xylem fiber length. Nat Biotechnol **44:** 255–266

**Esau K** (1965) Plant Anatomy. John Wiley & Sons, New York

**Fukuda H** (2004) Signals that control plant vascular cell differentiation. Nat Rev Mol Cell Biol **5:** 379–391

**Funk V, Kositsup B, Zhao C, Beers EP** (2002) The Arabidopsis xylem peptidase XCP1 is a tracheary element vacuolar protein that may be a papain ortholog. Plant Physiol **128:** 84–94

**Gallois JL, Woodward C, Reddy GV, Sablowski R** (2002) Combined SHOOT MERISTEMLESS and WUSCHEL trigger ectopic organogenesis in Arabidopsis. Development **129:** 3207–3217

**Galweiler L, Guan C, Muller A, Wisman E, Mendgen K, Yephremov A, Palme K** (1998) Regulation of polar auxin transport by AtPIN1 in Arabidopsis vascular tissue. Science **282:** 2226–2230

**Gardiner JC, Taylor NG, Turner SR** (2003) Control of cellulose synthase complex localization in developing xylem. Plant Cell **15:** 1740–1748

**Glawischnig E, Hansen BG, Olsen CE, Halkier BA** (2004) Camalexin is synthesized from indole-3-acetaldoxime, a key branching point between primary and secondary metabolism in Arabidopsis. Proc Natl Acad Sci USA **101:** 8245–8250

**Gray-Mitsumune M, Mellerowicz EJ, Abe H, Schrader J, Winzell A, Sterky F, Blomqvist K, McQueen-Mason S, Teeri TT, Sundberg B** (2004) Expansins abundant in secondary xylem belong to subgroup A of the alpha-expansin gene family. Plant Physiol **135:** 1552–1564

**Guo FO, Young J, Crawford NM** (2003) The nitrate transporter AtNRT1.1 (CHL1) functions in stomatal opening and contributes to drought susceptibility in Arabidopsis. Plant Cell **15:** 107–117

**Guo Y, Cai Z, Gan S** (2004) Transcriptome of Arabidopsis leaf senescence. Plant Cell Environ **27:** 521–549

**Hardtke CS, Berleth T** (1998) The Arabidopsis gene MONOPTEROS encodes a transcription factor mediating embryo axis formation and vascular development. EMBO J **17:** 1405–1411

**Haseloff J, Dormand EL, Brand AH** (1999) Live imaging with green fluorescent protein. Methods Mol Biol **122:** 241–259

**Hawker NP, Bowman JL** (2004) Roles for Class III HD-Zip and KANADI genes in Arabidopsis root development. Plant Physiol **135:** 2261–2270

**Hull AK, Vij R, Celenza JL** (2000) Arabidopsis cytochrome P450s that catalyze the first step of tryptophan-dependent indole-3-acetic acid biosynthesis. Proc Natl Acad Sci USA **97:** 2379–2384

**Husebye H, Chadchawan S, Winge P, Thangstad OP, Bones AM** (2002) Guard cell- and phloem idioblast-specific expression of thioglucoside glucohydrolase 1 (myrosinase) in Arabidopsis. Plant Physiol **128:** 1180–1188

**Inoue T, Higuchi M, Hashimoto Y, Seki M, Kobayashi M, Kato T, Tabata S, Shinozaki K, Kakimoto T** (2001) Identification of CRE1 as a cytokinin receptor from Arabidopsis. Nature **409:** 1060–1063

**Jang JC, Fujioka S, Tasaka M, Seto H, Takatsuto S, Ishii A, Aida M, Yoshida S, Sheen J** (2000) A critical role of sterols in embryonic patterning and meristem programming revealed by the fackel mutants of Arabidopsis thaliana. Genes Dev **14:** 1485–1497

**Jefferson RA, Kavanagh TA, Bevan MW** (1987) GUS fusions: beta-glucuronidase as a sensitive and versatile gene fusion marker in higher plants. EMBO J **6:** 3901–3907

**Jeong S, Trotochaud AE, Clark SE** (1999) The Arabidopsis CLAVATA2 gene encodes a receptor-like protein required for the stability of the CLAVATA1 receptor-like kinase. Plant Cell **11:** 1925–1933

**Kang HG, Foley RC, Onate-Sanchez L, Lin CGT, Singh KB** (2003) Target genes for OBP3, a Dof transcription factor, include novel basic helix-loop-helix domain proteins inducible by salicylic acid. Plant J **35:** 362–372

**Kang HG, Singh KB** (2000) Characterization of salicylic acid-responsive, Arabidopsis Dof domain proteins: overexpression of OBP3 leads to growth defects. Plant J **21:** 329–339

**Karpinska B, Karlsson M, Srivastava M, Stenberg A, Schrader J, Sterky F, Bhalerao R, Wingsle G** (2004) MYB transcription factors are differentially expressed and regulated during secondary vascular tissue development in hybrid aspen. Plant Mol Biol **56:** 255–270

**Kerstetter RA, Bollman K, Taylor RA, Bomblies K, Poethig RS** (2001) KANADI regulates organ polarity in Arabidopsis. Nature **411:** 706–709

**Kirst M, Johnson AF, Baucom C, Ulrich E, Hubbard K, Staggs R, Paule C, Retzel E, Whetten R, Sederoff R** (2003) Apparent homology of expressed genes from wood-forming tissues of loblolly pine (*Pinus taeda* L.) with Arabidopsis thaliana. Proc Natl Acad Sci USA **100:** 7383–7388

**Klucher KM, Chow H, Reiser L, Fischer RL** (1996) The AINTEGUMENTA gene of Arabidopsis required for ovule and female gametophyte development is related to the floral homeotic gene APETALA2. Plant Cell **8:** 137–153

**Kondratieva-Melville EA, Vodolazsky LE** (1982) Morphological and anatomical structure of Arabidopsis thaliana (Brassicaceae) in ontogenesis. Bot J **67:** 1060–1069

**Koroleva OA, Davies A, Deeken R, Thorpe MR, Tomos AD, Hedrich R** (2000) Identification of a new glucosinolate-rich cell type in Arabidopsis flower stalk. Plant Physiol **124:** 599–608

**Kroymann J, Textor S, Tokuhisa JG, Falk KL, Bartram S, Gershenzon J, Mitchell-Olds T** (2001) A gene controlling variation in Arabidopsis glucosinolate composition is part of the methionine chain elongation pathway. Plant Physiol **127:** 1077–1088

**Lev-Yadun S** (1994) Induction of sclereid differentiation in the pith of Arabidopsis thaliana (L.) Heynh. J Exp Bot **45:** 1845–1849

**Mahonen AP, Bonke M, Kauppinen L, Riikonen M, Benfey PN, Helariutta Y** (2000) A novel two-component hybrid molecule regulates vascular morphogenesis of the Arabidopsis root. Genes Dev **14:** 2938–2943

**McConnell JR, Emery J, Eshed Y, Bao N, Bowman J, Barton MK** (2001) Role of PHABULOSA and PHAVOLUTA in determining radial patterning in shoots. Nature **411:** 709–713

**Milioni D, Sado PE, Stacey NJ, Roberts K, McCann MC** (2002) Early gene expression associated with the commitment and differentiation of a plant tracheary element is revealed by cDNA-amplified fragment length polymorphism analysis. Plant Cell **14:** 2813–2824

**Mizukami Y, Fischer RL** (2000) Plant organ size control: AINTEGUMENTA regulates growth and cell numbers during organogenesis. Proc Natl Acad Sci USA **97:** 942–947

**Motose H, Sugiyama M, Fukuda H** (2004) A proteoglycan mediates inductive interaction during plant vascular development. Nature **429:** 873–878

**Naur P, Petersen BL, Mikkelsen MD, Bak S, Rasmussen H, Olsen CE, Halkier BA** (2003) CYP83A1 and CYP83B1, two nonredundant cytochrome P450 enzymes metabolizing oximes in the biosynthesis of glucosinolates in Arabidopsis. Plant Physiol **133:** 63–72

**Nazoa P, Vidmar JJ, Tranbarger TJ, Mouline K, Damiani I, Tillard P, Zhuo DG, Glass AD, Touraine B** (2003) Regulation of the nitrate transporter gene AtNRT2.1 in Arabidopsis thaliana: responses to nitrate, amino acids and developmental stage. Plant Mol Biol **52:** 689–703

**Oh S, Park S, Han KH** (2003) Transcriptional regulation of secondary growth in Arabidopsis thaliana. J Exp Bot **54:** 2709–2722

**Ooka H, Satoh K, Doi K, Nagata T, Otomo Y, Murakami K, Matsubara K, Osato N, Kawai J, Carninci P, et al** (2003) Comprehensive analysis of NAC family genes in Oryza sativa and Arabidopsis thaliana. DNA Res **10:** 239–247

**Oono Y, Chen QG, Overvoorde PJ, Kohler C, Theologis A** (1998) Age mutants of Arabidopsis exhibit altered auxin-regulated gene expression. Plant Cell **10:** 1649–1662

**Orsel M, Krapp A, Daniel-Vedele F** (2002) Analysis of the NRT2 nitrate transporter family in Arabidopsis. Structure and gene expression. Plant Physiol **129:** 886–896

**Patzlaff A, McInnis S, Courtenay A, Surman C, Newman LJ, Smith C, Bevan MW, Mansfield S, Whetten RW, Sederoff RR, et al** (2003) Characterisation of a pine MYB that regulates lignification. Plant J **36:** 743–754

**Paux E, Tamasloukht M, Ladouce N, Sivadon P, Grima-Pettenati J** (2004) Identification of genes preferentially expressed during wood formation in Eucalyptus. Plant Mol Biol **55:** 262–280

**Quackenbush J** (2002) Microarray data normalization and transformation. Nat Genet (Suppl) **32:** 496–501

**Redman JC, Haas BJ, Tanimoto G, Town CD** (2004) Development and evaluation of an Arabidopsis whole genome Affymetrix probe array. Plant J **38:** 545–561

**Riechmann JL, Heard J, Martin G, Reuber L, Jiang C, Keddie J, Adam L, Pineda O, Ratcliffe OJ, Samaha RR, et al** (2000) Arabidopsis transcription factors: genome-wide comparative analysis among eukaryotes. Science **290:** 2105–2110

**Ruiz-Medrano R, Xoconostle-Cazares B, Lucas WJ** (2001) The phloem as a conduit for inter-organ communication. Curr Opin Plant Biol **4:** 202–209

**Sablowski RW, Meyerowitz EM** (1998) A homolog of NO APICAL MERISTEM is an immediate target of the floral homeotic genes APETALA3/PISTILLATA. Cell **92:** 93–103

**Scheres B, Dilaurenzio L, Willemsen V, Hauser MT, Janmaat K, Weisbeek P, Benfey PN** (1995) Mutations affecting the radial organization of the Arabidopsis root display specific defects throughout the embryonic axis. Development **121:** 53–62

**Schoof H, Lenhard M, Haecker A, Mayer KFX, Jurgens G, Laux T** (2000) The stem cell population of Arabidopsis shoot meristems is maintained by a regulatory loop between the CLAVATA and WUSCHEL genes. Cell **100:** 635–644

**Schrader J, Nilsson J, Mellerowicz EJ, Berglund A, Nilsson P, Hertzberg M, Sandberg G** (2004) A high-resolution transcript profile across the wood-forming meristem of poplar identifies potential regulators of cambial stem cell identity. Plant Cell **16:** 2278–2292

**Souer E, van Houwelingen A, Kloos D, Mol J, Koes R** (1996) The no apical meristem gene of petunia is required for pattern formation in embryos and flowers and is expressed at meristem and primordia boundaries. Cell **85:** 159–170

**Stadler R, Sauer N** (1996) The Arabidopsis thaliana AtSUC2 gene is specifically expressed in companion cells. Bot Acta **109:** 299–306

**Steinmann T, Geldner N, Grebe M, Mangold S, Jackson CL, Paris S, Galweiler L, Palme K, Jurgens G** (1999) Coordinated polar localization of auxin efflux carrier PIN1 by GNOM ARF GEF. Science **286:** 316–318

**Sterky F, Regan S, Karlsson J, Hertzberg M, Rohde A, Holmberg A, Amini B, Bhalerao R, Larsson M, Villarroel R, et al** (1998) Gene discovery in the wood-forming tissues of poplar: analysis of 5,692 expressed sequence tags. Proc Natl Acad Sci USA **95:** 13330–13335

**Takada S, Hibara K, Ishida T, Tasaka M** (2001) The CUP-SHAPED COTYLEDON1 gene of Arabidopsis regulates shoot apical meristem formation. Development **128:** 1127–1135

**Takei K, Ueda N, Aoki K, Kuromori T, Hirayama T, Shinozaki K, Yamaya T, Sakakibara H** (2004) AtIPT3 is a key determinant of nitrate-dependent cytokinin biosynthesis in Arabidopsis. Plant Cell Physiol **45:** 1053–1062

**Talbert PB, Adler HT, Parks DW, Comai L** (1995) The REVOLUTA gene is necessary for apical meristem development and for limiting cell divisions in the leaves and stems of Arabidopsis thaliana. Development **121:** 2723–2735

**Taylor NG, Howells RM, Huttly AK, Vickers K, Turner SR** (2003) Interactions among three distinct CesA proteins essential for cellulose synthesis. Proc Natl Acad Sci USA **100:** 1450–1455

**Taylor NG, Scheible WR, Cutler S, Somerville CR, Turner SR** (1999) The irregular xylem3 locus of Arabidopsis encodes a cellulose synthase required for secondary cell wall synthesis. Plant Cell **11:** 769–779

**Terol J, Bargues M, Perez-Alonso M** (2000) ZFWD: a novel subfamily of plant proteins containing a C3H zinc finger and seven WD40 repeats. Gene **260:** 45–53

**Thelander M, Fredrikkson D, Schouten J, Hoge JH, Ronne H** (2002) Cloning by pathway activation in yeast: identification of an Arabidopsis thaliana F-box protein that can turn on glucose repression. Plant Mol Biol **49:** 69–79

**Timpte C, Lincoln C, Pickett FB, Turner J, Estelle M** (1995) The AXR1 and AUX1 genes of Arabidopsis function in separate auxin-response pathways. Plant J **8:** 561–569

**Todd J, Post-Beittenmiller D, Jaworski JG** (1999) KCS1 encodes a fatty acid elongase 3-ketoacyl-CoA synthase affecting wax biosynthesis in Arabidopsis thaliana. Plant J **17:** 119–130

**Tran LS, Nakashima K, Sakuma Y, Simpson SD, Fujita Y, Maruyama K, Fujita M, Seki M, Shinozaki K, Yamaguchi-Shinozaki K** (2004) Isolation and functional analysis of Arabidopsis stress-induced NAC transcription factors that bind to a drought-responsive *cis*-element in the *early responsive to dehydration stress 1* promoter. Plant Cell **16:** 2481–2498

**Vilaine F, Palauqui JC, Amselem J, Kusiak C, Lemoine R, Dinant S** (2003) Towards deciphering phloem: a transcriptome analysis of the phloem of Apium graveolens. Plant J **36:** 67–81

**Vroemen CW, Mordhorst AP, Albrecht C, Kwaaitaal MA, de Vries SC** (2003) The CUP-SHAPED COTYLEDON3 gene is required for boundary and shoot meristem formation in Arabidopsis. Plant Cell **15:** 1563–1577

**Weir I, Lu JP, Cook H, Causier B, Schwarz-Sommer Z, Davies B** (2004) CUPULIFORMIS establishes lateral organ boundaries in Antirrhinum. Development **131:** 915–922

**Williams J, Phillips AL, Gaskin P, Hedden P** (1998) Function and substrate specificity of the gibberellin 3 beta-hydroxylase encoded by the Arabidopsis GA4 gene. Plant Physiol **117:** 559–563

**Xie Q, Frugis G, Colgan D, Chua NH** (2000) Arabidopsis NAC1 transduces auxin signal downstream of TIR1 to promote lateral root development. Genes Dev **14:** 3024–3036

**Ye ZH** (2002) Vascular tissue differentiation and pattern formation in plants. Annu Rev Plant Biol **53:** 183–202

**Ye ZH, Varner JE** (1996) Induction of cysteine and serine proteases during xylogenesis in Zinnia elegans. Plant Mol Biol **30:** 1233–1246

**Zhao C, Johnson BJ, Kositsup B, Beers EP** (2000) Exploiting secondary growth in Arabidopsis. Construction of xylem and bark cDNA libraries and cloning of three xylem endopeptidases. Plant Physiol **123:** 1185–1196

**Zhong RQ, Ye ZH** (2004) Amphivasal vascular bundle 1, a gain-of-function mutation of the IFL1/REV gene, is associated with alterations in the polarity of leaves, stems and carpels. Plant Cell Physiol **45:** 369–385